# Synthesis and Photochemistry of a Photolabile Precursor of *N*-Methyl-D-Aspartate (NMDA) That Is Photolyzed in the Microsecond Time Region and Is Suitable for Chemical Kinetic Investigations of the NMDA Receptor†

Kyle R. Gee,‡ Li Niu,§,⊥ Klaus Schaper,§,# Vasanthi Jayaraman,|| and George P. Hess*,§

*Molecular Probes, Inc., 4849 Pitchford Ave., Eugene, Oregon 97402, and Section of Biochemistry, Molecular and Cell Biology, Division of Biological Sciences, 216 Biotechnology Building, Cornell University, Ithaca, New York, 14853-2703*

*Received November 9, 1998*

ABSTRACT: The amino acid L-glutamate is a major neurotransmitter at excitatory synapses within the central nervous system. Neuronal responses to glutamate are mediated by at least three receptor types, one of which is the NMDA subtype, named for its specific ligand *N*-methyl-D-aspartic acid. Neurotransmitter receptors are transmembrane proteins that can form ion channels upon binding a specific ligand and are involved in many physiological activities of the brain and in some neurological disorders. Elucidating the mechanisms of the formation of transmembrane receptor-channels and of receptor regulation and inhibition is necessary for understanding nervous system function and for designing potential therapeutic agents. This has been hampered by the lack of rapid reaction techniques suitable for investigating protein-mediated reactions on cell surfaces. Recently a laser-pulse photolysis technique was developed to study the chemical reactions of channel-forming receptor proteins in the microsecond-to-millisecond time region. To apply the technique to NMDA[1] receptors a photolabile NMDA precursor ($\beta$-DNB NMDA) was synthesized. In this precursor the side chain carboxylate was protected as a photosensitive 2,2′-dinitrobenzhydryl ester. Photolysis with 308 nm laser light generated free NMDA with a time constant of $4.2 \pm 0.1$ $\mu$s at pH 7 and a photolysis quantum yield of $0.18 \pm 0.05$. In rat hippocampal neurons the $\beta$-DNB NMDA (250 $\mu$M) neither activated endogenously expressed receptors nor potentiated or inhibited the NMDA response. Equilibration of hippocampal neurons in the whole-cell current recording mode with 250 $\mu$M caged precursor followed by a pulse of 333 nm laser light resulted in a rapid current rise with a rate constant of 100 $s^{-1}$ due to opening of NMDA-activated receptor-channels. The caged NMDA precursor described here now makes it possible to investigate the mechanism of NMDA receptors in the micro- to millisecond time region.

The amino acid L-glutamate is a major neurotransmitter at excitatory synapses within the central nervous system (*1*). Neuronal responses to glutamate appear to be mediated by at least three different receptor types, one of which is the NMDA[1] subtype, named for its specific ligand *N*-methyl-D-aspartic acid (*2*, *3*). The receptors are transmembrane proteins that on binding a specific neurotransmitter can form transient transmembrane channels which conduct inorganic ions. They are involved in many physiological activities of the brain (*4*, *5*) and in some neurological disorders (*3*, *6*). Elucidation of the mechanisms of the formation, regulation, and inhibition of transmembrane receptor-channels is required for understanding fundamental nervous system function and for designing potential therapeutic agents. Investigations of the mechanisms have been hampered by the lack of rapid reaction techniques suitable for studying reactions on cell surfaces (*7*−*11*). Ongoing efforts are aimed at developing new methods for this purpose (reviewed in refs *10* and *11*).

Photolabile ("caged") precursors of biologically active substances (*12*) have become important tools for the study of rapid biological events (reviewed in refs *10*, *13*, and *14*). In theory, photolysis of a system containing a caged compound can release the active parent compound with much better spatial and temporal resolution than is normally attained with conventional mixing methods, which were designed for studying reactions in solution (*15*). There exist both theoretical reasons (*16*) and experimental evidence (*7*, *10*) that conventional mixing techniques are inadequate for kinetic investigations of many reactions on cell surfaces. Diffusional delays in kinetic investigations of cell surface

† This work was supported by Grant GM 04842 from the National Institute of General Medical Science (G.P.H). K.S. was supported by a Fellowship from Deutsche Forschungsgellschaft, and V.J. by a Fellowship from the Cancer Research Fund of the Damon-Runyon-Walter Winchell Foundation.

* Address correspondence to this author. Tel: (607) 255-4809; fax: (607) 255-2428. E-mail: gph2@cornell.edu.

‡ Molecular Probes, Inc.

§ Cornell University.

⊥ Present address: Departments of Biology and Chemistry, Massachusetts Institute of Technology, Cambridge, MA 02139.

# Present address: Institut für Organische Chemie und Makromoleculare Chemie, Heinrich-Heine Universität Düsseldorf, Germany.

|| Present address: Department of Chemistry, Marquette University, Milwaukee, WI 53201-1881.

[1] Abbreviations: CNB, α-carboxy-2-nitrobenzyl; DNB, 2, 2′-dinitrobenzhydryl; GABA, $\gamma$-aminobutyric acid; NMDA, *N*-methyl-D-aspartic acid; TFA, trifluoroacetic acid; TLC, thin-layer chromatography.

10.1021/bi9826557 CCC: $18.00 
Published on Web 02/17/1999

neurotransmitter receptors are avoided by using caged neurotransmitters (*8*). Caged neurotransmitters suitable for investigating the excitatory acetylcholine (*8*), glutamate (*17*−*19*), and kainate (*20*) receptors and the inhibitory γ-aminobutyric acid (*21*) and glycine (*22*) receptors have been synthesized and characterized, both photochemically and biologically. The spatial resolution aspect of reagent application afforded by the use of caged compounds is also being exploited, in fields as diverse as neuronal synaptic connection in tissue slices (*23*), receptor mapping in single cells (*24*), and in a circuit of cells controlling a measurable response in the nematode *Caenorhabditis elegans* (*25*), the study of cytoskeleton dynamics (*26*), and large-scale fluid dynamics (*27*, *28*).

In practice, the synthesis of a new caged compound does not guarantee that the precursor will be useful in the intended application. Several criteria must normally be met, the first of which is that the caged compound must be biologically inactive and stable in the system of interest. In the case of caged neurotransmitters (*8*; reviewed in refs *10*, *11*, and *29*), this means that neither the caged version nor the photolysis side products must inhibit or potentiate an agonist response and that in the dark cells or tissue bathed in solutions of caged neurotransmitter are stable, e.g., there is no hydrolysis to free neurotransmitter. Next, the caged compound must be soluble in the cell buffer used, and photolysis in an acceptable wavelength range (normally 300−400 nm) must result in an uncaging event of sufficient speed and product quantum yield. Receptor activation kinetics must be measured on the millisecond (or faster) time scale, so photolysis of caged neurotransmitters must occur in the microsecond regime. Photolysis rates and yields are highly dependent on the leaving group, the caging group, and the bonding between the two. At present there are insufficient data for one to predict a priori that a new caged compound will photolyze with a particular rate and yield, so each new compound synthesized must be characterized thoroughly before actual use. Additionally, a not uncommon occurrence is to find that a new caged neurotransmitter photolyzes well but when applied to cells is biologically active before photolysis and is, therefore, of suboptimal utility (e.g., see ref *19*).

Several caged neurotransmitters have been prepared and used successfully to investigate receptor mechanisms in cells and membrane fragments (reviewed in refs *10*, *11*, *29*, and *49*). Introduction of the α-carboxy-2-nitrobenzyl (CNB) group in the caging of carbamoylcholine (*8*) resulted in a photolabile precursor that met all criteria listed above. (Carbamoylcholine is a stable analogue of acetylcholine.) The CNB group is a variation on the *o*-nitrobenzyl caging group, by far the most widely used photolabile protecting group, and has been used in the caging of glycine (*30*), glutamate (*18*), GABA (*21*), and kainic acid (*20*). In caged carbamoylcholine and caged glycine, the CNB group was attached to the nitrogen atoms, whereas for caged glutamate, GABA, and kainic acid the most useful versions had the CNB group attached to oxygen atoms of carboxylates. However, when the CNB group was attached to the side chain carboxylate of NMDA, the resulting caged probe was biologically active before photolysis, although it photolyzed well (NMDA production on the order of 30 μs and quantum yield of 0.43) (*19*). Efforts to attach the CNB group to the α-carboxylate or the nitrogen atom of NMDA did not result in the desired product (K. R. Gee, unpublished observations).

The 2,2′-dinitrobenzhydryl (DNB) caging group has been used successfully as a photolabile group on phosphates (*31*) and carboxylates (*32*). Attachment of this more bulky caging group to NMDA was anticipated to more significantly interfere with receptor interaction such that the DNB-caged NMDA would be inert, unlike the CNB-caged NMDA (*19*). Here we report the synthesis and characterization of such a caged NMDA, β-(2,2′-dinitrobenzhydrol)-caged (DNB) NMDA (**5**). We demonstrate that DNB-caged NMDA meets all of the criteria necessary for successful applications to the study of NMDA receptor activation mechanisms.

## MATERIALS AND METHODS

*Bis-α,β-O-(2,2′-dinitrobenzhydryl)-N-tert-butoxycarbonyl-N-methyl-*D*-aspartate (**3**).* A mixture of *N-t*-BOC NMDA (**1**) (*19*) (0.17 g, 0.69 mmol), 2,2′-dinitrobenzhydrol (**2**) (*33*) (387 mg, 1.41 mmol), EDC·HCl (287 mg, 1.5 mmol), and catalytic amounts of 4-(dimethylamino)pyridine and *N*-hydroxybenzotriazole in dichloromethane (12 mL) was prepared at −78 °C. The reaction mixture was allowed to warm to room temperature with stirring in darkness. More EDC·HCl (0.10 g) was added, and stirring was continued for 24 h. The reaction mixture was partitioned between ethyl acetate (40 mL) and water (30 mL). The organic layer was washed with brine (1×), dried (sodium sulfate), and concentrated to 0.55 g of an off-white foam. This foam was purified by flash chromatography (*34*) to give the bis-ester **3** as 0.28 g (54%) of a pale yellow powder: $^1$H NMR ($CDCl_3$) δ 8.1 (m, 4H), 7.91 (m, 2H), 7.55 (m, 8H), 7.36 (m, 3H), 7.14 (m, 1H), 4.92 (t, $J$ = 6.8 Hz, 1H), 3.16 (m, 1H), 2.97 (m, 1H), 2.80 (s, 3H), 1.4 (s, 9H). Anal. Calcd for $C_{36}H_{33}N_5O_{14}$: C, 56.92; H, 4.38; N, 9.22. Found: C, 56.84; H, 4.67; N, 8.87.

*β-O-(2,2′-Dinitrobenzhydryl)-N-tert-butoxycarbonyl-N-methyl-*D*-aspartic Acid (**4**).* To a pale brown solution of bis-ester **3** (0.27 g, 0.6 mmol) in dioxane (4 mL) at room temperature was added NaOH (15 mg, 0.37 mmol) as a solution in 1.0 mL of water. The resulting mixture was stirred in darkness for 24 h, and the pH was lowered to 4.5 with AcOH. Concentration gave 0.35 g of a light yellow oil which was purified via flash chromatography to give starting bis-ester **3** as 27 mg (10%), and the mono-ester **4** as 70 mg (39%) of a pale brown clear oil: $^1$H NMR ($CDCl_3$) 8.07 (m, 2H), 7.90 (br s, 1H), 7.52 (m, 4H), 7.31 (m, 2H), 7.16 (m, 2H), 4.48 (t, $J$ = 6.5 Hz, 1H), 3.15 (m, 1H), 2.99 (dd, $J$ = 16.4, 7.8 Hz, 1H) 2.82 (s, 3H), 1.34 (s, 9H). Anal. Calcd for $C_{23}H_{25}N_3O_{10}$: C, 54.87; H, 5.01; N, 8.35. Found: C, 54.99; H, 5.19; N, 7.79.

*β-O-(2,2′-Dinitrobenzhydryl)-N-methyl-*D*-aspartic Acid, Trifluoroacetate (**5**).* To a pale brown solution of the mono-ester **4** (70 mg, 0.14 mmol) in dichloromethane (2 mL) under nitrogen at room temperature was added trifluoroacetic acid (1 mL). TLC after 15 min showed reaction completion. The volatiles were removed in vacuo, and toluene was stripped from the residue, leaving 80 mg of a pale brown solid. This solid was purified by chromatography on Sephadex LH-20 using water/acetone as eluant, giving the title compound as 40 mg (56%) of a colorless powder after concentration; during concentration about half of the trifluoroacetic acid counterion was volatilized: $^1$H NMR (DMSO-$d_6$) δ 8.12 (dd,

$J$ = 7.9, 2.7 Hz, 2H), 7.79 (m, 2H), 7.68 (m, 4H), 7.49 (d, $J$ = 8.0, 1.0 Hz, 1H), 3.46 (t, $J$ = 6.4 Hz, 1H), 2.97 (dd, $J$ = 16.5, 6.4 Hz, 1H), 2.79 (dd, $J$ = 16.5, 6.2 Hz, 1H), 2.45 (s, 3H); $^{19}$F (DMSO-$d_6$) 68.9. Anal. Calcd for $C_{18}H_{17}N_3O_8 \cdot 0.5CF_3CO_2H$: C, 50.02; H, 3.88; N, 9.27. Found: C, 50.26; H, 3.74; N, 9.37.

*Laser Flash Photolysis.* Due to the limited solubility of DNB−NMDA (**5**) in water, solutions containing 20% DMSO were used. DNB−NMDA (0.65 mg, 1.6 mmol) was dissolved in DMSO (400 mL) to yield a 4 mM solution. This solution was slowly added to water (600 mL) to create a 1.6 mM solution of DNB−NMDA in water/DMSO (60/40) and then diluted 1:1 with different buffers (200 mM) to give the desired 0.8 mM solution of DNB−NMDA in 100 mM buffer containing 20% DMSO.

The instrumentation used for the experiments has been described in detail before (*8*). Briefly, solutions of DNB−NMDA (0.8 mM) were placed in a 10 mm × 2 mm quartz cuvette and were photolyzed with 40 mJ pulses of 308 nm (XeCl) light from an excimer laser (Lumonics TE 861 M). The transient intermediate **6** was observed at right angles to the photolysis beam using a halogen lamp (Newport model 780) with a Corning WGS360 cutoff filter, a monochromator (0.3 m McPherson 275 single pass), and a photomultiplier (Thorn EMI9635QB). The signal was amplified with a preamplifier (Thorn EMI model A1) and recorded with a Tektronix TDS 310 digital Oscilloscope and stored to file through the serial port of a 286 computer. The signals were digitized at a rate of 2 MHz. The recorded traces were analyzed using a nonlinear least-squares analysis procedure (*39*) in the MicroCal software Origin 3.5. All transient absorptions could be fitted to a single-exponential decay. The intermediate spectra were measured in 10 nm wavelength steps between 380 and 580 nm. All measurements were done at pH 7, using 100 mM Tris buffer. The decay rates of the *aci*-nitro intermediate (assumed to be identical to the rate of product formation) (*35*−*38*) were measured at a wavelength of 470 nm, close to the maximum of the intermediate absorption. The following buffers were used: pH 3.8 acetate (100 mM), pH 7.0 Tris (100 mM), and pH 10.6 glycine (100 mM).

*Product Quantum Yield.* The quantum yield was determined essentially as described before (*8*). The apparatus described above was used. The laser energy absorbed by the sample solution was measured simultaneously to the recording of the photolysis traces with a joule meter (ballistic thermopile, Gentec ED-200) behind the cuvette and recorded with an oscilloscope (LeCroy Scope Station 140). The solution of DNB−NMDA was photolyzed with a number of consecutive laser shots. The traces were recorded at 470 nm, and the measurements were done at pH 7 (100 mM Tris). With the assumption that the amount of released NMDA is proportional to the amount of intermediate formed (*35*−*38*), the amount of released NMDA can be calculated by using the following equations (*8*):

$$A_n = \epsilon_m l c_o \phi K_E \exp[-(\phi K_E F(n-1)] \quad (1)$$

$$\ln A_n = \ln(\epsilon_m l c_o \phi K_E) - \phi K_E F(n-1) \quad (2)$$

$A_n$ is the intermediate absorbance after the $n$th laser shot, $\epsilon_m$ is the molar extinction coefficient, $l$ is the path length for the observing light, $c_o$ is the initial concentration, and $\phi$ is the quantum yield. $K_E$ is the ratio of the number of photons absorbed in each laser shot to the number of molecules in the target beam, $F$ is the fraction of solution through which the laser beam passed, and $n$ is the number of laser pulses used. The product $K_E F$ is given by the ratio of the total number of photons absorbed in each laser shot to the total number of molecules in the cuvette. This product can be obtained easily, and it is constant because the absorbed amount of laser light is constant in all laser shots (4.6 mJ). To achieve this, the sample has to be photolyzed at a wavelength close to the isosbestic point of **5** and the photoproduct **7**.

*Cell Culture and Whole-Cell Recording.* The protocol for preparing the hippocampal neurons used in the measurements was previously described (*20*) and is similar to the one described by Patneau et al. (*40*). Briefly, hippocampal neurons were obtained from two day-old Sprague-Dawly rats and cultured on 35 mm Falcon dishes pretreated with collagen and in 5% $CO_2$. Minimal Eagle's medium was supplemented with 10 mM glucose, 2.7 mM glutamine, 5% fetal bovine serum, and horse serum on the first day; on the second day, 5% fetal bovine serum was omitted (all from GIBCO). On the third day, the cells were treated with 41 $\mu$M 5-fluoro-2′-deoxyuridine and 102 mM uridine (final concentration; all from Sigma) for 24−48 h. The cells used in experiments were from 1 to 3 weeks old. For the measurements, a cell was lifted from the bottom of a culture dish using the electrode and suspended in the external solution (see below). The cell body had a diameter of about 15 $\mu$m and a capacitance of about 7 pF. Electrodes were made with a List L/M-3P-A pipet puller and fire-polished using a Narishige MF-83 polisher. The electrode resistance was about 3 MΩ. The extracellular solution consisted of 145 mM NaCl, 3 mM KCl, 1 mM $CaCl_2$, 10 mM glucose, and 10 mM HEPES (pH 7.4), and the solution for filling the electrode consisted of 140 mM CsCl, 1 mM $CaCl_2$, 10 mM EGTA, and 10 mM HEPES (pH 7.2). A cell-flow device (*41*, *42*) was used to equilibrate receptors on the cell surface with ligands, NMDA (Sigma), and caged NMDA. Whole-cell currents (*43*) were detected with a List L/M-EPC-7 amplifier, filtered through a low-pass RC filter (Krohn-Hite 3322) with a cutoff frequency of 2 kHz (−3 dB point), and recorded with a sampling frequency of 300−500 Hz by a Labmaster DMA digitizer (Scientific Solutions) driven by the PClamp program (Axon). The Origin 3.5 Program (MicroCal Software) was used for fitting and plotting data.

*Laser-Pulse Photolysis*. All of the compounds, including caged NMDA and NMDA, were dissolved in the extracellular buffer. A Candela SLL 500 flash-lamp-pumped dye laser with sulforhodamine 640 (Exciton) as the laser dye was used for all of the laser-pulse photolysis measurements. Single laser pulses at 333 nm, tuned by a secondary harmonic generator, were coupled into an optical fiber (core diameter 200, SFS200/220N, FiberGuide Industries) and directed to the cells with the output energy of 500 $\mu$J from the end of the fiber as measured by a joule meter (Gentec ED-200). Triggering of the laser pulse and data collection were synchronized with the timing capabilities of the Labmaster DMA hardware (Scientific Solutions) driven by the PClamp program (Axon Instruments). The whole-cell current generated by released NMDA was detected and recorded as

Scheme 1

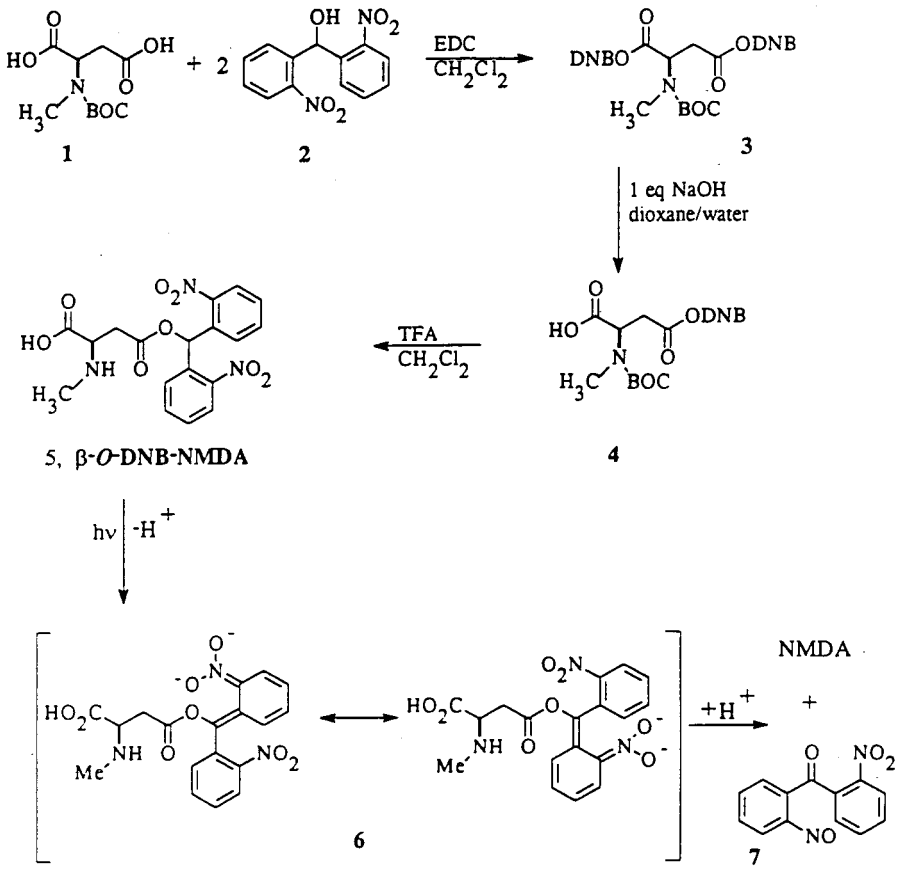


described previously (*8*). The response of the neuron to known concentrations of NMDA was determined using the cell-flow method (*42*) before and after photolysis of caged NMDA. This served two purposes: (i) to detect cell or receptor damage and (ii) to determine the concentration of free NMDA released. The concentration of free NMDA released was determined by comparing the corrected current amplitudes obtained in cell-flow experiments (*42*) (i.e., standard curves obtained with free NMDA) and the maximum current amplitude obtained in the laser-pulse photolysis experiment. In the laser-pulse photolysis experiments, the cutoff frequency from the filter was 10−20 kHz and the sampling frequency was set to 10−50 kHz. The rising phase of the whole-cell current generated by photoreleased NMDA followed a single-exponential rate equation over 85% of the reaction (*9*, *45*):

$$I_t = I_{max}[1 - \exp(-k_{obs}t)] \quad (3a)$$

$$k_{obs} = k_{cl} + k_{op}[L/(L + K_1)]^2 \quad (3b)$$

$I_t$ is the current observed at time $t$, and $I_{max}$ is the maximum amplitude of the observed current in the absence of desensitization. $k_{obs}$ is the observed first-order rate constant for the channel opening process; $k_{op}$ and $k_{cl}$ are the rate constants for channel opening and closing, respectively. $L$ represents the concentration of the activating ligand (i.e., NMDA), and $K_1$ is the observed dissociation constant of this ligand from the receptor site controlling channel opening.

## RESULTS

*Synthesis.* Both carboxylates of *N-t*-BOC NMDA (**1**) (*19*) were esterified with 2,2′-dinitrobenzhydrol (**2**) (*33*). The α-carboxylate was selectively unmasked by treatment with a limited amount of hydroxide (*19*); esters of the side chain carboxylate are expected to be more hydrolytically stable than esters of the α-carboxylate (*18*, *19*). The resulting ester **4** was deprotected by brief treatment with trifluoroacetic acid, giving **5** as a colorless powder (Scheme 1).

*Photolysis.* The photochemical reaction leading to the release of free NMDA was characterized by transient absorbance spectroscopy. In vitro photolysis experiments were performed using DNB−NMDA (**5**) at 0.8 mM in the presence of 20% DMSO; 100 mM buffers used were pH 3.8 acetate, pH 7 Tris, and pH 10.6 glycine. An absorption maximum at 265 nm was measured for **5**, with an extinction coefficient of 16 900 $M^{-1}$ $cm^{-1}$. This is a much higher absorptivity than is attained when the standard *o*-nitrobenzyl caging groups are used. The photochemical reaction was initiated by irradiation of **5** with a single 10 ns laser pulse from a XeCl excimer laser at 308 nm and an energy of approximately 40 mJ per pulse. Figure 1 shows the absorbance change at 460 nm of **5** (at pH 7) upon photolysis. The appearance and disappearance of an absorbing species correspond to the expected *aci*-nitro intermediate **6**, the decay of which is thought to lead directly to free amino acid production (Scheme 1) (*36*−*38*). Additionally we ascertained that irradiation of **5** with a hand-held TLC illumination lamp produced free NMDA, as determined by coelution with a sample of authentic NMDA on an analytical TLC plate (data not shown). We also ascertained that the response of hippocampal neurons to 100 μM NMDA, determined by the cell-flow technique (*42*), is abolished in the presence of 200 μM MK-801 (data not shown), a specific inhibitor of the receptor (*46*, *47*).

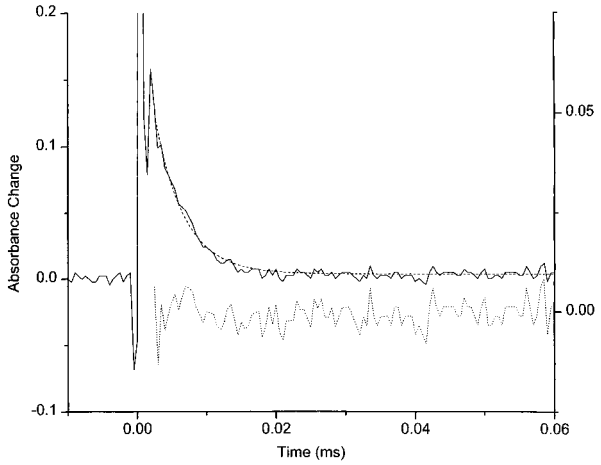


FIGURE 1: Absorption transient observed in the photolysis of **5** at 460 nm produced by a 10 ns laser flash at 308 nm (XeC1 excimer laser) in a 0.8 mM solution of **5** in 100 mM Tris, 20% DMSO, pH 7, and 22 °C. The single-exponential absorbance decay has a time constant of 4.2 ± 0.1 $\mu$s. The solid line represents the measured data and the dotted line the fitted curve. The lower panel gives the residuals of the fit (*40*). The absorbance change observed at zero time is produced by discharge of the laser power supply and is also observed in the absence of caged NMDA.

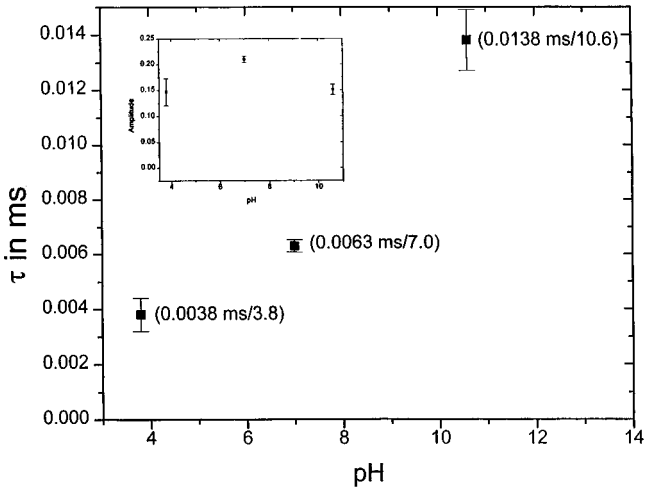


FIGURE 2: pH dependence of the time constant for the photolysis of DNB−NMDA (**5**). For all measurements, 0.8 mM solutions were photolyzed in buffer and 20% DMSO, using an excimer laser at 308 nm (XeCl) at 22 °C. The intermediate (**6**) spectra were recorded at 470 nm. The solutions were buffered with 100 mM acetate at pH 3.8, 100 mM Tris at pH 7 and 100 mM glycine at pH 10.6. Inset: pH dependence of the amplitude of the transient absorbance for the photolysis of DNB−NMDA using the conditions given above.

The time constant for the absorption decay is 4.2 ± 0.1 $\mu$s, determined by fitting the single-exponential curve. The symmetry of the *aci*-nitro intermediate obtained may explain why the decay seen following photolysis of **5** can be fitted with a single exponential curve, whereas double exponentials are normally required to fit decay curves after photolysis of unsymmetrical α-carboxy-2-nitrobenzyl (CNB) esters (*18*−*20*). This photolysis rate is about 5 times faster than the rates observed with previously prepared CNB esters of amino acid neurotransmitters (*18*−*21*).

The time constant for the release of NMDA from **5** is pH dependent. Figure 2 shows the pH dependence of the *aci*-nitro (**6**) decay time constant. The time constant decreases to 3.8 $\mu$s at pH 3.8 and increases to 13.8 $\mu$s at pH 10.6. In contrast, the observed amplitude for the formation of the *aci*-nitro intermediate, considered to be proportional to the concentration of photoreleased product (*36*−*38*), changes in the observed pH range by only a small amount (inset, Figure 2).

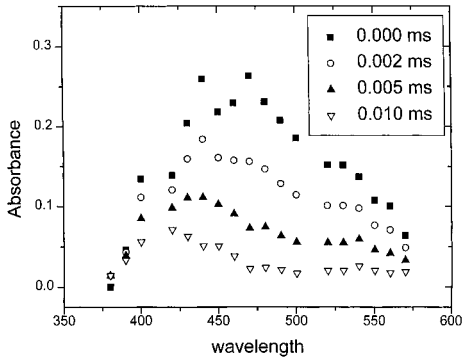


FIGURE 3: Intermediate spectra of **6** (0.8 mM in 100 mM Tris buffer, 20% DMSO) at pH 7 and 22 °C. The filled squares represent the intermediate spectra immediately after irradiation with laser light; the open circles represent the intermediate spectra at $t = 2$ $\mu$s, the filled triangles at $t = 5$ $\mu$s, and the open triangles at $t = 10$ $\mu$s.

Figure 3 shows the spectral distribution of the *aci*-nitro transient species (**6**) absorbance at various times after the laser pulse. The spectra are characteristic of the *aci*-nitro intermediates observed in the photolysis of *o*-nitrobenzyl derivatives (*35*, *36*). The absorption maximum at ca. 460 nm is red-shifted 30 nm from that observed when CNB esters are photolyzed (*8*, *18*, *20*, *21*), presumably because of the extended conjugation in the *aci*-nitro intermediate afforded by the second *o*-nitrobenzyl group. Figure 4 shows a plot of the logarithm of the transient amplitude as a function of the number of laser shots. From the slope, the photolysis quantum yield was determined to be 0.18 ± 0.05. The intercept gives an estimate of the transient absorbance extinction coefficient (ca. 810 $M^{-1}$ $cm^{-1}$ at 450 nm).

*Biological Characterization.* DNB−NMDA (**5**) was found to be inactive before photolysis on cultured rat hippocampal neurons. Solutions of **5** with concentrations as high as 250 $\mu$M can be achieved in external buffer without adding DMSO. The compound was stable under these condition; DNB−NMDA (**5**) (250 $\mu$M) dissolved in extracellular solution for 1 h at room temperature did not elicit a current response in hippocampal neurons in cell-flow measurements (*42*) (data not shown). Figure 5 shows that **5** did not potentiate or inhibit the NMDA response; the whole-cell currents measured upon application of 20 $\mu$M NMDA in the absence and presence of 250 $\mu$M **5** (preincubated with the cell for 10 s) were the same. The current amplitudes, rise times, and decay rates are the same within experimental error. The tests were recorded at −60 mV, pH 7.4, and ambient temperature. Note that 20 $\mu$M NMDA is not the saturating concentration (reported $EC_{50}$ values are in the 10−20 $\mu$M range) (*44*). Similar results were obtained in experiments using 100 $\mu$M NMDA (data not shown). In contrast, when $\beta$-CNB NMDA (300 $\mu$M), a previously synthesized and different caged NMDA derivative, was preincubated with hippocampal neurons for 5 s and tested in an experiment such as the one shown in Figure 5, it was found to inhibit the NMDA receptor (*19*).

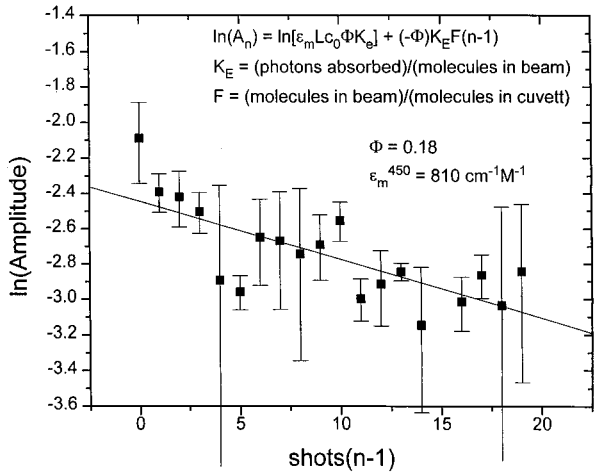


FIGURE 4: Determination of the product quantum yield for the photolysis of DNB−NMDA (**5**) in 100 mM Tris buffer (20% DMSO) at pH 7 and 22 °C. A cuvette containing 0.8 mM **5** was irradiated, with mixing of the solution between the laser pulses of 308 nm wavelength (50 mJ). The absorbed laser energy and the transient absorbance were monitored at 460 nm wavelength as a function of the number of laser shots. The ratio of photons absorbed to the number of molecules in the cuvette ($K_EF$) was 0.18, the path length ($L$) was 10 mm, and the fraction of volume irradiated ($F$) was estimated to be 0.25. The product quantum yield ($\Phi$) is defined as the number of NMDA molecules released divided by the number of photons absorbed. It was calculated from these data to be 0.18 ± 0.05; the absorbance of the intermediate was estimated to be 810 $M^{-1}$ $cm^{-1}$. The data represent the mean of two measurements, and the error bars represent the standard deviation.

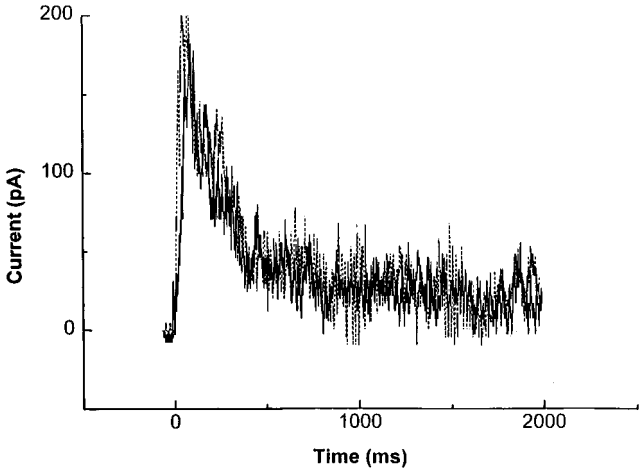


FIGURE 5: Whole-cell current responses of a rat hippocampal neuron to 20 $\mu$M NMDA in the absence (solid line) or presence (dashed line) of 250 $\mu$M DNB−NMDA at −60 mV, pH 7.4, and 22 °C (see Materials and Methods section). The experiments were done using the cell-flow technique (*42*) and the same cell. The experiment shown is representative of two others in which different cells were used. The corrected current amplitudes of the whole-cell currents induced by 20 $\mu$M NMDA in the absence and presence of 250 $\mu$M DNB−NMDA are 255 pA and 210 pA, respectively. Receptor desensitization, represented by the decreasing phase, proceeded in two phases. For the control (solid line), the rate of the fast phase is 37 $s^{-1}$ (31%) and of the slower phase 4.5 $s^{-1}$ (69%). In the presence of 250 $\mu$M DNB−NMDA (dashed line), the rate of the fast phase is 37 $s^{-1}$ (26%), and that of the slower phase is 4.2 $s^{-1}$ (74%). In this experiment, the cell was preincubated with 250 $\mu$M DNB−NMDA for 10 s before the application of 20 $\mu$M NMDA.

Photolysis of cells incubated with solutions of **5** resulted in a rapid rise in the whole-cell current, due to activation of the NMDA receptor channels by photoreleased NMDA. Figure 6 shows the whole-cell current recorded upon photolysis of a cell bathed in a 250 $\mu$M solution of **5**, giving an apparent concentration of 35 $\mu$M free NMDA. The rising phase of the whole-cell current represents the opening of ion channels activated by NMDA. A single-exponential fit to the rising phase gives a rate constant of 100 ± 10 $s^{-1}$, with a maximum current of 110 pA. Cell-flow experiments with a standard concentration of NMDA (20 $\mu$M) were performed before and after the photolysis to ascertain whether the cell or receptors were damaged in the laser-pulse photolysis experiments. Additionally, we ascertained that in experiments in which 1 mM caged NMDA was equilibrated with the cell surface receptors before photolysis (results not shown), in the presence of 100 $\mu$M MK-801, a specific inhibitor of the NMDA receptor (*46*, *47*), the observed current due to opening of receptor-channels was completely blocked.

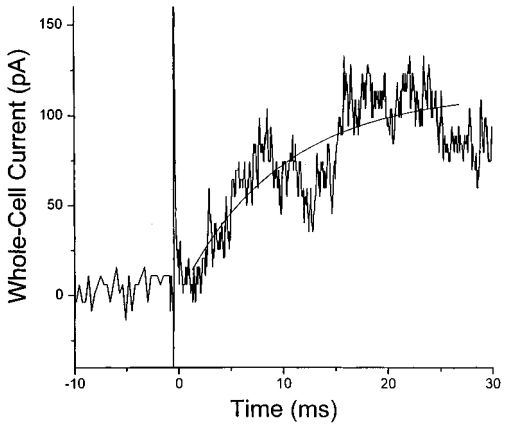


FIGURE 6: Whole-cell current recorded from a rat hippocampal neuron and generated by laser-pulse photolysis of 250 $\mu$M DNB−NMDA at −60 mV, pH 7.4, and 22 °C. The cell was preincubated with 250-$\mu$M DNB−NMDA for 400 ms. At time zero, a 600-ns pulse of 333-nm laser light with an energy output of 500 $\mu$J was fired. The spike at time zero is an instrument artifact. The concentration of free NMDA released from 250 $\mu$M caged NMDA under this condition was estimated to be 35 $\mu$M as calibrated by the cell-flow technique using known concentrations of NMDA solutions. The rising phase of the whole-cell current represents the opening of ion channels activated by NMDA. The solid line is a single-exponential fit to the rising phase of the current, using eq 3. The maximum current amplitude is 110 pA, and the rate constant for this process is 100 $s^{-1}$. This value is based on duplicate experiments with each of two different cells.

## DISCUSSION

The DNB caging group was recently shown by Baldwin et al. (*31*) to have considerable promise as an efficiently removed photoprotecting group on phosphates. Our previous efforts to develop caged versions of NMDA have not been completely successful, as the resulting compounds were active before photolysis (e.g., $\beta$-CNB−NMDA) (*19*). Would a bulkier caging group than the CNB group prevent interaction of caged NMDA with the receptor? Since the photolysis properties of the DNB group seemed promising, and it was expected that the DNB group when attached to NMDA would provide more structural perturbation than the CNB group, the synthesis of a DNB-caged NMDA was undertaken and its properties characterized.

The most expeditious route to such a molecule involved esterification of one of the carboxylic acid groups present in NMDA with 2,2′-dinitrobenzhydrol. Esters of the side chain carboxylate of aspartic acid derivatives are expected to be much more hydrolytically stable than corresponding esters of the α-carboxylate. Hydrolysis of the former is mediated by formation of a four-membered ring resulting from attack of the lone pair of electrons on the amine nitrogen on the ester carbonyl carbon, whereas hydrolysis of the latter involves formation of a three-membered ring. Compounds that produce four-membered rings during hydrolysis are much more stable than those that produce three-membered rings (*22*, *48*). Thus, both carboxylates of *N*-*t*-BOC NMDA were esterified with 2,2′-dinitrobenzhydrol, and the greater hydrolytic lability of the α-ester was exploited by treatment of the resulting bis-ester (**3**) with 1 equiv of hydroxide, resulting in selective cleavage of the α-ester ester. Simple treatment of the resulting mono-ester **4** with TFA cleaved the *tert*-butylcarbamate to give DNB−NMDA (**5**).

Photolysis of solutions of **5** generated a species that was characterized spectroscopically (Figure 3); it had the characteristics of the *aci*-nitro anion **6** intermediate commonly observed upon photolysis of *o*-nitrobenzyl compounds (*14*, *36*, *37*). The intermediate **6** obtained from **5** had an absorption maximum at 460 nm, which is red-shifted about 30 nm from *aci*-nitro intermediates obtained from photolysis of simpler *o*-nitrobenzyl compounds. Presumably this red-shift is a result of the extended conjugation of the *aci*-nitro intermediate due to the second *o*-nitrobenzyl moiety in the DNB-caging group. Decay of *aci*-nitro intermediates is thought to lead directly to free neurotransmitter production. The decay of **6** had a time constant of 4.2 ± 0.1 μs. This decay rate is about 5 times faster than that observed for CNB esters (vide ante), enabling kinetic processes to be investigated with a better time resolution. The rate of decay of **6** is dependent upon pH, increasing slightly at lower pH. Such behavior is consistent with general *o*-nitrobenzyl photochemistry, in which decay of *aci*-nitro intermediates is the rate-determining step and involves reaction with a proton (*14*).

A critical test of **5** was biological inertness before photolysis. Indeed, the compound at concentrations up to 250 μM neither induced any response on cultured rat hippocampal neurons nor potentiated or inhibited the NMDA response. The second nitrophenyl moiety in the DNB group moderates aqueous solubility relative to the CNB caging group, and thus DMSO was needed if concentrations of **5** higher than 250 μM were to be achieved in external buffer. Photolysis of cells incubated with solutions of **5** resulted in a rapid rise in the whole-cell current, a result of activation of ion channels associated with the NMDA receptor by photoreleased NMDA. Thus, DNB−NMDA (**5**) satisfies all of the stringent criteria required of caged compounds for utility in biological systems. It is, therefore, now possible to investigate the mechanism of NMDA receptors in the micro- to millisecond time region using the caged NMDA derivative described here.

## ACKNOWLEDGMENT

We thank Dr Gerald Feigenson for use of the diode array spectrophotometer and Susan Coombs for technical editorial work.

## REFERENCES

1. Jonas, P., & Spruston, N. (1994) *Curr. Opin. Neurobiol. 4*, 366−372.
2. Gasic, G. D., & Hollman, M. (1992) *Annu. Rev. Physiol. 54*, 507−536.
3. Hollmann, M., & Heinemann, S. (1994) *Annu. Rev. Neurosci. 17*, 31−108.
4. Collingridge, G. L., & Lester, R. A. J. (1989) *Pharmacol. Rev. 41*, 143−210.
5. Kandel, D. R., Schwartz, J. H, & Tessel, T. M. (1991) *Principles of Neurosciences*, 3rd ed., Elsevier, NY.
6. Greenmayre, J. T. (1986) *Arch. Neurol. 43*, 1058−1063.
7. Hess, G. P., Udgaonkar, J. B., & Olbricht, W. L. (1987) *Annu. Rev. Biophys. Biophys. Chem. 16*, 507−534.
8. Milburn, T., Matsubara, N., Billington, A. P., Udgaonkar, J. B., Walker, J. W., Carpenter, B. K., Webb, W. W., Marque, J., Denk, W., McCray, J. A., & Hess, G. P. (1989) *Biochemistry 28*, 49−55.
9. Matsubara, N., Billington, A. P., & Hess, G. P. (1992) *Biochemistry 31*, 5507−5514.
10. Hess, G. P. (1993) *Biochemistry 32*, 989−1000.
11. Hess, G. P., & Grewer, C. (1998) *Methods Enzymol. 291*, 443−473.
12. Kaplan, J. H. Forbush, B., & Hoffman, J. F. (1978) *Biochemistry 17*, 1929−1935.
13. Adams, S. R., & Tsien, R. Y. (1993) *Annu. Rev. Physiol. 55*, 755−783.
14. Corrie, J. E. T., & Trentham, D. R. (1993) in *Bioorganic Photochemistry* (Morrison, J., Ed.), Vol. 2, pp 243−305, Wiley, New York.
15. Gutfreund, H. (1995) *Kinetics for the Life Sciences: Receptors, Transmitters and Catalysts*, Cambridge University Press, Cambridge, UK.
16. Landau, V. G., & Lifshitz, E. H. (1959) *Fluid Mechanics*, Pergamon Press, Oxford, UK.
17. Wilcox, M., Viola, R. W., Johnson, K. W., Billington, A. P., Carpenter, B. K., McCray, J. A., Guzikowski, A., & Hess, G. P. (1990) *J. Org. Chem. 55*, 1585−1589.
18. Wieboldt, R., Gee, K. R., Niu, L., Ramesh, D., Carpenter, B. K., & Hess, G. P. (1994) *Proc. Natl. Acad. Sci. U.S.A. 91*, 8752−8756.
19. Gee, K. R., Niu, L., Schaper, K., & Hess, G. P. (1995) *J. Org. Chem. 60*, 4260−4263.
20. Niu, L., Gee, K. R., Schaper, K., & Hess, G. P. (1996) *Biochemistry 35*, 2030−2036.
21. Gee, K. R., Wieboldt, R., & Hess, G. P. (1994) *J. Am. Chem. Soc. 116*, 8366−8367.
22. Niu, L., Wieboldt, R., Ramesh, D., Carpenter, B. K., & Hess, G. P. (1996) *Biochemistry 35*, 8136−42.
23. Katz, L. C., & Dalva, M. B. (1994) *J. Neurosci. Methods 54*, 205−218.
24. Denk, W. (1994) *Proc. Natl. Acad. Sci. U.S.A. 91*, 6629−6633.
25. Li, H., Avery, L., Denk, W., & Hess, G. P. (1997) *Proc. Natl. Acad. Sci. U.S.A. 94*, 5912−5916.
26. Theriot, J. A., & Mitchison, T. J. (1991) *Nature 352*, 126−131.
27. Lempert, W., Magee, K., Ronney, P., Gee, K. R., & Haugland, R. P. (1995) *Exper. Fluids 18*, 249−257.
28. Guilkey, J. E., Gee, K. R., McMurtry, P. A., & Klewicki, J. C. (1996) *Exper. Fluids 21*, 237−242.
29. Nerbonne, J. M. (1996) *Curr. Opin. Neurobiol. 6*, 379−386.
30. Billington, A. P., Walstrom, K. M., Ramesh, D., Guzikowski, A. P., Carpenter, B. K., & Hess, G. P. (1992) *Biochemistry 31*, 5500−5507.
31. Baldwin, J. E., McConnaughie, A. W., Moloney, M. G., Pratt, A. J., & Shim, S. B. (1990) *Tetrahedron 46*, 6879−6884.
32. Patchornik, A., Amit, B., & Woodward, R. B. (1970) *J. Am. Chem. Soc. 92*, 6333−6335.
33. Johns, R. B., & Markham, K. R. (1962) *J. Chem. Soc.*, 3712−3717.
34. Still, W. C., Kahn, M., & Mitra, A. (1978) *J. Org. Chem. 43*, 2923−2925.

35. McCray, J. A., Herbette, L., Kihara, T., & Trentham, D. R. (1980) *Proc. Natl. Acad. Sci. U.S.A. 77*, 7273−7241.
36. Schupp, H., Wong, W. K., & Schnabel, W. (1987) *J. Photochem. 36*, 85−97.
37. Walker, J. W., Reid, G. P., McCray, J. A., & Trentham, D. R. (1988) *J Am. Chem. Soc. 110*, 7170−7177.
38. Wootton, J. F., & Trentham, D. R. (1989) *NATO Adv. Study Inst. Ser. C 272*, 277−296.
39. Bevington, P. R. (1969) *Data Reduction and Error Analysis for the Physical Sciences*, McGraw-Hill, New York.
40. Patneau, D. K., Vyklicky, L., Jr., & Mayer, M. L. (1993) *J. Neurosci. 13*, 3496−3509.
41. Krishtal, O. A., & Pidoplichko, V. I. (1980) *Neuroscience 5*, 2325−2327.
42. Udgaonkar, J. B., & Hess, G. P. (1987) *Proc. Natl. Acad. Sci. U.S.A. 84*, 8758−8762.
43. Hamill, O. P., Marty, E., Neher, E., Sakmann, B., & Sigworth, F. J. (1981) *Pfluegers Arch. 391*, 85−100.
44. Krishtal, O. A., Osipchuk, Y. V., & Vrublevsky. S. V. (1988) *Neurosci. Lett. 84*, 271−276.
45. Niu, L., & Hess, G. P. (1993) *Biochemistry 32*, 3831−3835.
46. Wong, E. H. F., Kemp, J. A., Priestley, T., Knight, A. R., Woodruff, G. N., & Iversen, L. L. (1986) *Proc. Natl. Acad. Sci. U.S.A. 84*, 7104−7108.
47. Halliwell, R. F., Peters, J. A., & Lambert, J. J. (1989) *Br. J. Pharmacol. 96*, 480−494.
48. Carey, F. A., & Sundberg, R. J. (1990) *Advanced Organic Chemistry*, 3rd ed., pp 305−313, Plenum, New York.
49. Gee, K. R., Carpenter, B. K., and Hess, G. P. (1998) *Methods Enzymol. 291*, 30−50.

BI9826557